Using Spaceborne Synthetic Aperture Radar to Improve Marine Surface Analyses

KAREN S. FRIEDMAN

Caelum Research Corporation, Camp Springs, Maryland

TODD D. SIKORA

Department of Oceanography, United States Naval Academy, Annapolis, Maryland

WILLIAM G. PICHEL AND PABLO CLEMENTE-COLÓN

NOAA/National Environmental Satellite, Data, and Information Service, Camp Springs, Maryland

GARY HUFFORD

NOAA/National Weather Service Forecast Office, Anchorage, Alaska

28 June 2000 and 6 December 2000

ABSTRACT

The ever-changing weather and lack of in situ data in the Bering Sea warrants experimentation with new meteorological observing systems for this region. Spaceborne synthetic aperture radar (SAR) is well suited for observing the sea surface footprints of marine meteorological phenomena because its radiation is sensitive to centimeter-scale sea surface roughness, regardless of the time of day or cloud conditions. The near-surface wind field generates this sea surface roughness. Therefore, the sea surface footprints of meteorological phenomena are often revealed by SAR imagery when the main modulator of sea surface roughness is the wind. These attributes, in addition to the relatively high resolution of SAR products, make this instrument an excellent candidate for filling the meteorological observing needs over the Bering Sea.

This study demonstrates the potential usefulness of SAR for observing Bering Sea meteorology by focusing on its ability to image the sea surface footprints of polar mesoscale cyclones (PMCs). These storms can form unexpectedly and are threatening to maritime interests. In this demonstration, a veteran meteorologist at the Anchorage National Weather Service Forecast Office is asked to produce a surface reanalysis for three separate archived cases when SAR imaged a PMC but the original analysis, produced without the aid of SAR data, did not display it. The results show that in these three cases the inclusion of SAR data in the analysis procedure leads to large differences between the original surface analysis and the reanalysis. Of particular interest is that, in each case, the PMC is added into the reanalysis. It is argued that the reanalyses more accurately portray the near-surface meteorology for each case.

1. Introduction

The Bering Sea is a semienclosed regional sea that separates eastern Russia from Alaska. The presence of a 500–800-km-wide continental shelf, extensive seasonal sea ice cover, and a convergence of nutrient-rich current systems (NRC 1996) are all factors contributing to the extraordinary productivity of this sea. The Bering Sea fishery has grown significantly over the last decade and presently it nets over 2 million tons annually, generating revenues in excess of $1.5 billion. This rich harvest has attracted vessels of all sizes to the Bering Sea in search of fish year-round. This includes the harsh winter months when intense weather systems, such as polar mesoscale cyclones (PMCs), move through the area.

PMCs are primarily a high-latitude phenomenon forming in the atmosphere above marine environments. Northern Hemisphere PMCs have been documented in such places as the Norwegian Sea, the Barents Sea, the Greenland Sea, the Labrador Sea, Hudson Bay, the Beaufort Sea, the Gulf of Alaska, the Bering Sea, the Sea of Japan, and much of the North Pacific Ocean (e.g., Businger 1985, 1987; Bond and Shapiro 1991; Albright et al. 1995; Douglas et al. 1995; Grønås and Kvamstø 1995; Mailhot et al. 1996; Heinemann and Claud 1997). In the Southern Hemisphere, polar mesoscale cyclones

Corresponding author address: Karen S. Friedman, NOAA, E/RA3, WWBG, Room 102, 5200 Auth Road, Camp Springs, MD 20746-4304.
E-mail: Karen.Friedman@noaa.gov

have been documented over much of the middle- and high-latitude Southern Ocean (Carrasco et al. 1997a,b; Carleton and Song 1997).

However, PMCs have also been documented well equatorward from polar regions, such as over the Great Lakes (Minor et al. 2000), the Mediterranean Sea (Rasmussen 1989), and off the west coast of the United States (Monteverdi 1976; Locatelli et al. 1982).

PMCs are defined as all meso-α-scale and meso-β-scale [using Orlanski's (1975) scale definitions] cyclonic vortices poleward of the major frontal zones. The term polar low refers to a subset of polar mesoscale cyclones whose near-surface wind speed exceeds 15 m s^{-1} and whose scale is up to 1000 km. They are therefore smaller than extratropical cyclones, and they have comparably shorter life cycles than an extratropical cyclone, with the time from their inception to death on the order of days. They primarily form from fall to spring and are routinely associated with strong winds, large fluxes of sensible and latent heat, and convective precipitation.

The continuously changing weather in the Bering Sea presents a major threat to life and property. This makes PMCs of particular interest to National Weather Service (NWS) marine meteorologists and to the U.S. maritime community. Vessels at sea have unexpectedly found themselves caught in one of these storms leading to damage of the vessel and sometimes to the death of its occupants. The NWS Forecast Office Anchorage (NWSFOA) is responsible for producing timely and accurate analyses, forecasts, and warnings for the Bering Sea. These primary products, issued three times per day, provide information on the extent of the winds and waves. However, the analyses, forecasts, and warnings often overlook threatening mesoscale weather conditions due to the lack of observations in and around the Bering Sea. The in situ data that are available are received from a few coastal cities, a few buoys, and ship reports.

Satellite sensors, such as the Geostationary Operational Environmental Satellite (GOES) imager and the Advanced Very High Resolution Radiometer, can be used to locate PMCs by passively sensing their cloud signatures. However, when there are multiple layers of clouds or when a PMC is embedded within a larger cloud deck, a PMC may not be visible (e.g., see case study 4 from Sikora et al. 2000). For this reason, an active sensor such as synthetic aperture radar (SAR) can be useful for detecting PMCs.

SAR has an advantage over passive sensors because it is sensitive to centimeter-scale sea surface roughness, regardless of the time of day or cloud conditions. The near-surface wind field generates this sea surface roughness. Therefore, the sea surface footprints of meteorological phenomena are often revealed by SAR imagery when the main modulator of sea surface roughness is the wind (see the comprehensive review in Mourad 1999). SAR is particularly useful for extracting fine-resolution low-level meteorological information that cannot be extracted from traditional remote sensing data. The SAR sensor on the Canadian satellite *RADARSAT-1* is currently used by the United States for ice and near-surface wind studies.

Chunchuzov et al. (2000) and Sikora et al. (2000) were the first refereed studies to investigate SAR's potential to aid in PMC detection and forecasting. We note, however, that currently SAR is not publicly available as a dedicated tool for operational meteorologists. It is the goal of this research to extend prior work and demonstrate the utility of SAR imagery in an operational meteorological setting. In this demonstration, a veteran meteorologist at NWSFOA was asked to produce a surface reanalysis for three separate archived cases when SAR imaged a PMC but the original analysis, produced without the aid of SAR data, did not display it.

This experiment served as an introduction to SAR for the NWSFOA. Beginning in October of 1999, they were provided with SAR-derived products as part of the two-year National Oceanic and Atmospheric Administration (NOAA) National Environmental Satellite, Data, and Information Service (NESDIS) Alaska SAR Demonstration (Pichel and Clemente-Colón 2000).

2. Synthetic aperture radar

Radars are active sensors that transmit microwave radiation in pulses and record the radiation backscattered in the direction of the sensor. The reflectivity function of the surface material determines how much of the energy gets reflected. Radar cross section (RCS) is a measure of the radiation that is scattered back and recorded by the sensor. The RCS is dependent on the roughness and the dielectric constant of the material, the local incidence angle, and the radar wavelength and polarization. The rougher and wetter a surface is, and the smaller the local incidence angle, the higher the RCS value.

SAR works by collecting data across a path that would be equivalent to the data collected by a large antenna. These data are processed to synthesize the pattern that a large antenna would see. For this to work, the sensor must record both the magnitude and phase of the received energy in order to correct the phase of the energy along the flight path before summing the received energy for each target. This involves complicated postprocessing before generating an image and therefore the imagery is not immediately available.

The measurements from SAR of RCS from the ocean are mainly the result of centimeter-scale Bragg scattering. This is caused by in-phase resonant scattering from surface waves with wavelengths similar to the radar wavelength, and is dependent on the amplitude of the Bragg waves and the tilt of the small region being measured. On the ocean, Bragg waves are created by the local wind and are propagated along the surface. The amplitude of the waves is dependent on local wind conditions and surface currents. The tilt of the region of

measurement is a result of the amplitude of long-scale waves from sources such as local winds and swell.

When a SAR image reveals a phenomenon such as an eddy or atmospheric storm, the forcing is only the effect that these phenomena have on the Bragg waves. SAR can image the effects of near-surface winds because changes in wind speed and direction change wave energy density, which is sensed at the Bragg scale. When interpreting SAR images, regions with higher winds will generally appear brighter than those with calm winds. The scatterometer is another active sensor that is used to measure wind fields on the ocean surface. The primary advantage of a SAR over a scatterometer is resolution. Most SARs have a nominal resolution on order 10 to 100 m while the resolution of most scatterometers is on order 10 km. SAR, therefore, can provide a much more detailed view of marine meteorological phenomena.

3. *RADARSAT-1*

The Canadian *RADARSAT-1* was launched in November 1995, into a sun-synchronous polar orbit with an ascending equator crossing time (local time) of 1800. It has a 5.6-cm C-band SAR with horizontal–horizontal polarization. The sensor mode used in this study is ScanSAR Wide B with a swathwidth of 480 km. The resolution of the original image data is 100 m with a pixel spacing of 50 m. However, the resolution used in this study is 200 m with a pixel spacing of 100 m. *RADARSAT-1* has the ability to revisit a spot within the Bering Sea region, at approximately 60° latitude, every 1–2 days. Much of the data taken for use by the United States are downloaded directly from the satellite to the Alaska SAR Facility in Fairbanks, Alaska. They in turn provide SAR data within approximately 6 h to users through the NOAA Satellite Active Archive. The authors acknowledge that for SAR to be considered for operational meteorological use, the time delay between data acquisition and dissemination must be decreased from 6 h. One also has the option of buying SAR data from commercial vendors. These vendors can typically provide data to the end user in a much more timely fashion. However, the cost is not trivial and may be out of the reach of many users.

4. Reanalysis experiment

Three case studies were conducted in this experiment. A lead forecaster at NWSFOA, with 27 years of experience in Alaska, produced synoptic surface reanalyses for each of the hours closest to the time of the SAR image. The regular duties of a lead forecaster are to coordinate the forecasts for aviation, marine, and the public so that they are all in agreement. They also are responsible for making the synoptic analysis chart for the other forecasters to use as a basis. These attributes led us to conduct the experiment using a lead forecaster at NWSFOA. In this experiment, the lead forecaster was directed to produce the reanalyses using the conventional data available for the original analyses as well as the SAR data. Conventional data included land-based surface observations, marine surface observations (buoy and ship), *GOES-9* visible and IR imagery, and *NOAA-12* visible and IR imagery when available. The results from this study are taken from the comparison between the original surface analysis made by the NWSFOA, and the reanalysis using the SAR data. Further SAR analysis of the same PMC cases is provided in Sikora et al. (2000).

5. Results

a. Case 1: 14 February 1998

The surface analysis in Fig. 1a for 1800 UTC on 14 February 1998 places a 992-hPa PMC at 55°N, 179°E. To the southwest of the PMC, a ship reported northwesterly winds at 30 kt. This direction is consistent with the cyclonic circulation expected around a PMC. To the southwest of the PMC, a synoptic-scale cyclone is shown at 46°N, 159°E. A ridge of high pressure sits to the east of the cyclone, along the date line.

Figure 1b is a SAR image of a PMC centered at 58°N, 175°E at 1843 UTC on 14 February 1998. This PMC lies to the northwest of the one originally analyzed by NWSFOA. The PMC is made evident by a sharp backscatter (wind) boundary that is shaped like a hook. The center of the storm has low backscatter and most likely low winds. Along the hooklike wind boundary, there are wavelike features, which may be caused by horizontal wind shear. Ice is apparent in the upper left-hand corner of the image and is brighter (higher backscatter) than the surrounding ocean surface. Roll vortices are imaged in the upper right-hand corner of the image as a series of parallel lines (Mourad 1996), leading to the speculation that the wind boundary is the manifestation of the leading edge of an arctic air mass propagating offshore. Recall that SAR can detect the presence of atmospheric phenomena such as roll vortices when the phenomena affect the ocean surface, thereby affecting the backscatter.

The introduction of the SAR imagery into the analysis process causes the meteorologist to place an additional PMC in the reanalysis (Fig. 1c) to the northwest of the PMC in the original analysis. The two PMCs are connected by a common trough axis and are surrounded by a common 996-hPa isobar. The pressure gradient in the vicinity of the newly analyzed PMC is significantly stronger than that presented on the original analysis. We argue, therefore, that for this case study, the addition of SAR data results in an analysis that provides a better representation of the danger present in the PMC area.

b. Case 2: 26 February 1998

The surface analysis at 0000 UTC 26 February 1998 (Fig. 2a), displays a very benign pressure gradient be-

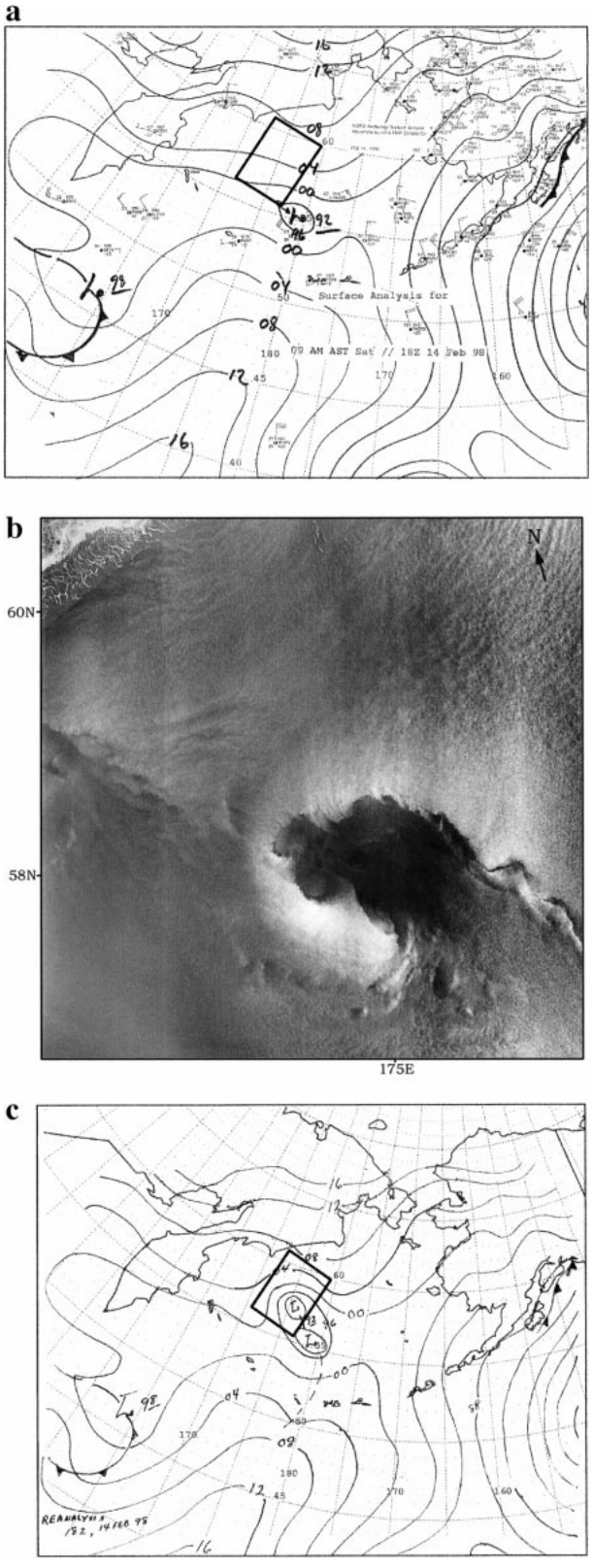

tween the three synoptic-scale cyclones centered at 55°N, 164°E; 63°N, 164°W; and 40°N, 176°W. The pressure gradient is indicative of weak winds between these three systems. There are very few surface reports in the region between 55° and 65°N in the central Bering Sea making it hard to infer the true conditions there.

The SAR image for 0550 UTC 26 February 1998 (Fig. 2b) shows three PMCs, all along a common wind boundary. The largest PMC is located in the bottom right-hand corner of the image and is centered at approximately 57°N, 180°. The region of higher backscatter and therefore winds is generally to the north of the PMC's semicircular boundary. The center of the PMC has calmer winds and appears darker in the SAR image. The second PMC is centered at 57.5°N, 177°E and the third, and smallest, PMC is just off the ice edge at 59.5°N, 175°E. Mottled areas can be seen in the lower-left corner of the image and are a manifestation of cellular convection (Sikora et al. 1995). The SAR signature of roll vortices can also be seen in the vicinity of the PMCs.

When the meteorologist uses the information from the SAR imagery to make the reanalysis (Fig. 2c), the changes are significant. The reanalysis has a PMC and surface troughs located in the region where SAR detected PMCs. Note the increased pressure gradient in the vicinity of the PMC in the reanalysis. Higher winds are expected in this region, but in the original analysis, low winds were suggested. Again, we argue from this that the addition of SAR data to the analysis procedures results in an analysis more telling of the actual surface conditions present in the SAR scene.

c. Case 3: 24 March 1998

The surface analysis for 1800 UTC 24 March 1998 (Fig. 3a) suggests a trough with a weak pressure gradient extending westward from the large synoptic-scale cyclone centered at 58°N, 164°W. The existing surface reports in the Bering Sea show strong winds, though reports are lacking above 57°N. The weak pressure gradient in the region between 55° and 60°N, and 177° and 170°E, would support the premise of lower winds in this region as opposed to elsewhere.

Figure 3b shows a PMC below the ice line at 1834 UTC. This PMC consists of a wind boundary coming from the east and wrapping counterclockwise into the center at 58.5°N, 173.5°E. Wavelike features are seen along this boundary, as in the previous cases. Higher

←

FIG. 1. (a) Surface analysis prepared by the National Weather Service Forecast Office Anchorage (NWSFOA) at 1800 UTC 14 Feb 1998. Complementary SAR image is outlined as a rectangle. (b) *RADARSAT-1* SAR image taken at 1843 UTC 14 Feb 1998. (Copyright Canadian Space Agency, 1998.) (c) Surface reanalysis prepared by NWSFOA at 1800 UTC 14 Feb 1998. Complementary SAR image is outlined as a rectangle.

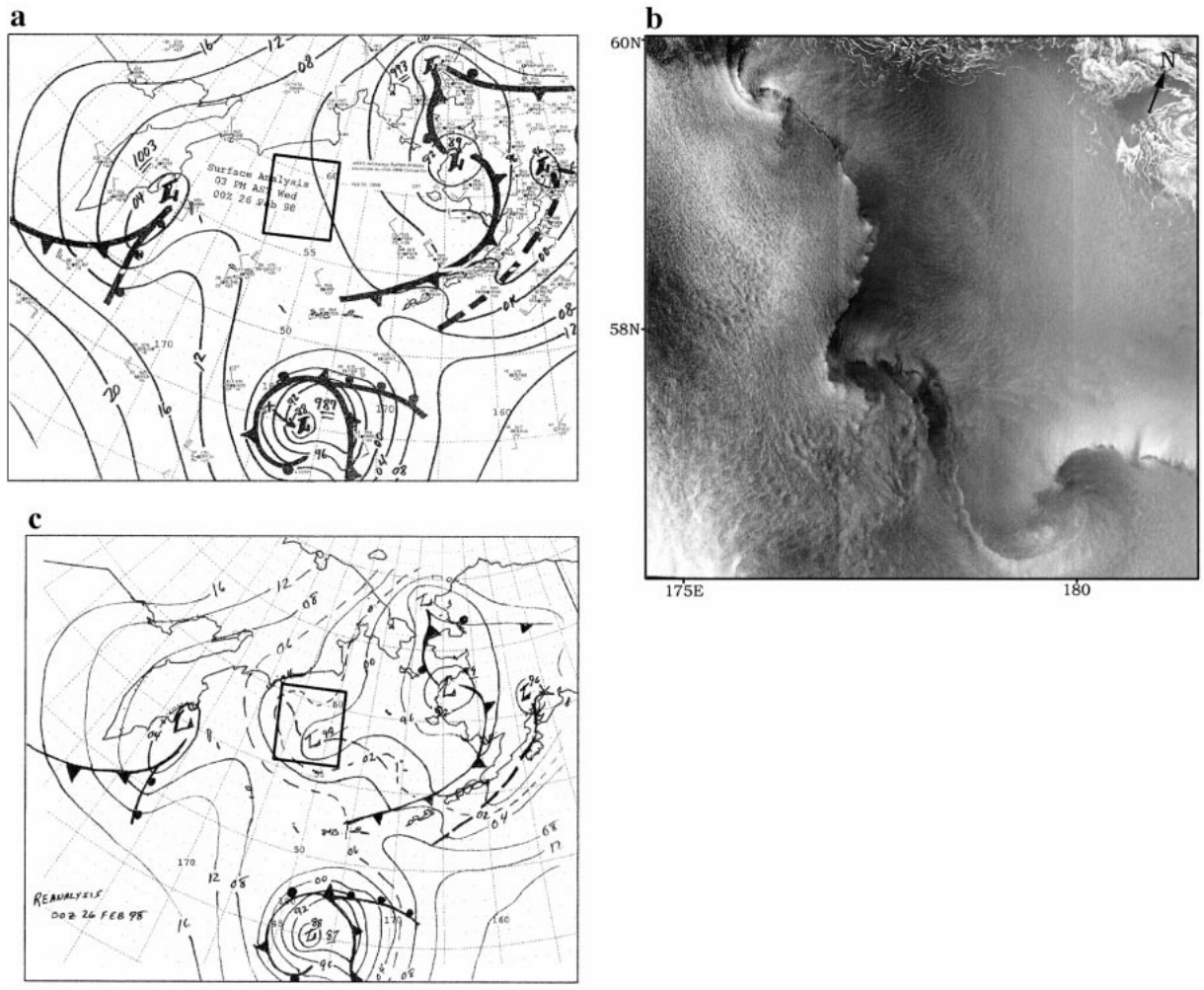

FIG. 2. (a) Surface analysis prepared by NWSFOA at 0000 UTC 26 Feb 1998. Complementary SAR image is outlined as a rectangle. (b) *RADARSAT-1* SAR image taken at 0550 UTC on 26 Feb 1998. (Copyright Canadian Space Agency, 1998.) (c) Surface reanalysis prepared by NWSFOA at 0000 UTC 26 Feb 1998. Complementary SAR image is outlined as a rectangle.

backscatter and therefore wind speed are found to the north of this boundary. A second wind boundary wraps toward the center from the west, with higher winds to the south. When the SAR image is used by the meteorologist to make the reanalysis found in Fig. 3c, a PMC is added at 58°N, 173°E and a trough of low pressure extends from the PMC to the east, along the wind boundary discussed above. This results in the tightening of the pressure gradient around the PMC where the gradient was previously weaker. The high winds associated with PMCs are more accurately represented in the reanalysis with this change in the pressure gradient.

6. Conclusions

This study attempts to demonstrate how useful SAR can be to the weather forecasting community. Though done on a small scale, and in a limited area, the results show that SAR has a potential to improve marine surface analyses by adding more information about the near-surface meteorological conditions. In all of the cases presented, the meteorologist at the NWSFOA made significant changes in the reanalysis after the addition of SAR data. The degree of change varied between cases, with the case on 26 February showing the largest difference.

Starting October 1999, the NWSFOA was given access to near-real-time SAR data and derived products for use in their analyses. The derived products are surface wind images and vectors (Monaldo 2000). The products offer the meteorologist more information than was provided to them in this study by giving wind speeds and direction in the area covered by the SAR image. For the NOAA/NESDIS Alaska SAR Demonstration, one to two passes are collected each day each in the Bering Sea and Gulf of Alaska. These passes cover a swath from approximately 50° to 70°N with a width of 480 km. Each pass shifts in longitude each day

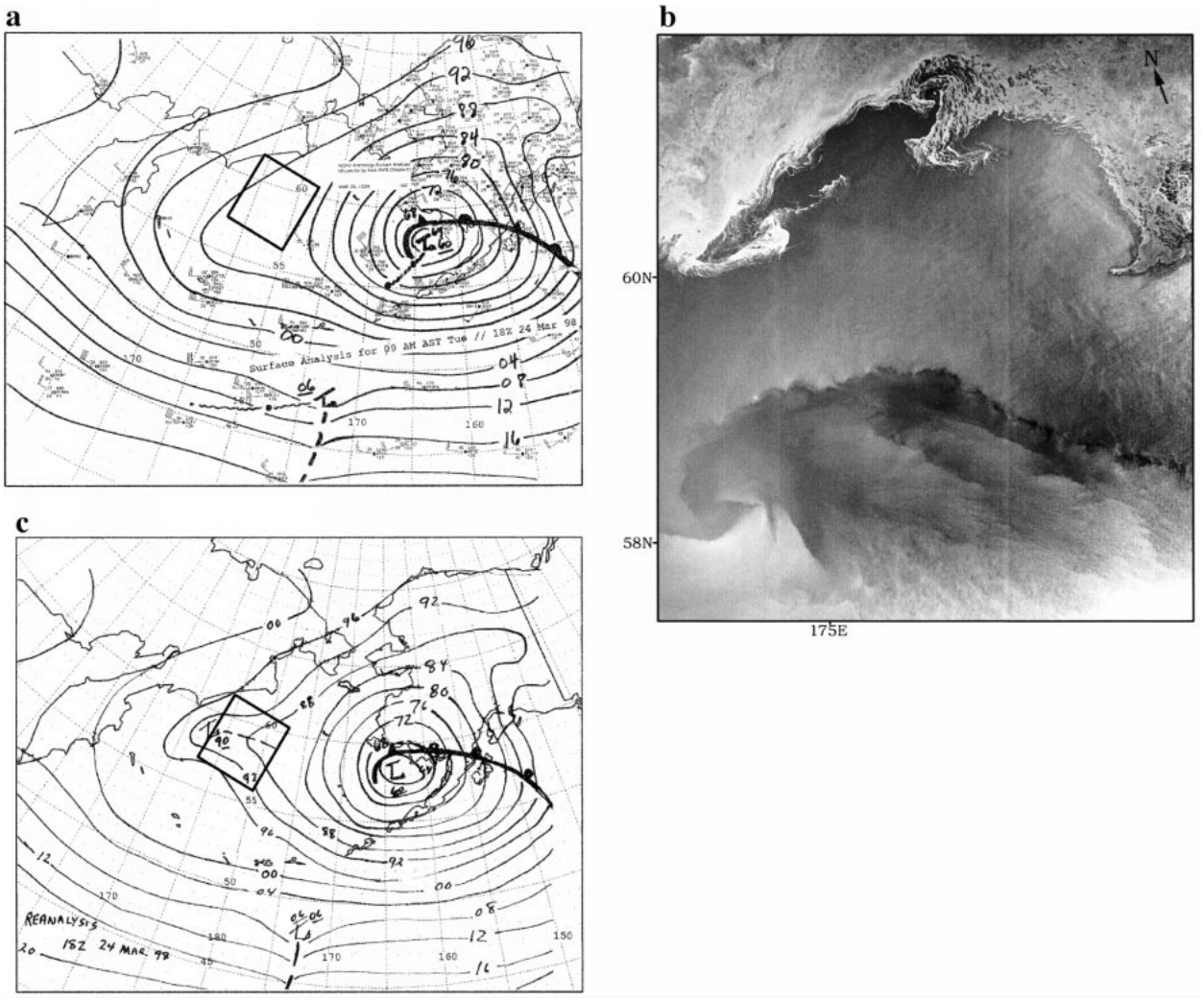

FIG. 3. (a) Surface analysis prepared by NWSFOA at 1800 UTC 24 Mar 1998. Complementary SAR image is outlined as a rectangle. (b) *RADARSAT-1* SAR image taken at 1834 UTC 24 Mar 1998. (Copyright Canadian Space Agency, 1998.) (c) Surface reanalysis prepared by NWSFOA at 1800 UTC 24 Mar 1998. Complementary SAR image is outlined as a rectangle.

for complete aggregate coverage of the region over the course of a week. Although the SAR data are not usually received in time to directly aid the forecast, they have been used in modifying forecasts and they provide insight into conditions that are taken into account in subsequent forecasts. In particular, insights into coastal wind variations and the location of PMCs have been of value.

Acknowledgments. *RADARSAT-1* data have been obtained under the NASA *RADARSAT-1* Application Development and Research Opportunity, Project 396. The authors wish to thank Frank Monaldo for his use of a detrending algorithm, Chris Wackerman for his help in SAR interpretation, and Don Finch, a lead forecaster at NWSFOA, for participating in this experiment.

REFERENCES

Albright, M. D., R. J. Reed, and D. W. Ovens, 1995: Origin and structure of a numerically simulated polar low over Hudson Bay. *Tellus,* **47A,** 834–848.

Bond, N. A., and M. A. Shapiro, 1991: Polar lows over the Gulf of Alaska in conditions of reverse shear. *Mon. Wea. Rev.,* **119,** 551–572.

Businger, S., 1985: The synoptic climatology of polar low outbreaks. *Tellus,* **37A,** 419–432.

——, 1987: The synoptic climatology of polar-low outbreaks over the Gulf of Alaska and the Bering Sea. *Tellus,* **39A,** 307–325.

Carleton, A. M., and Y. Song, 1997: Synoptic climatology, and intrahemispheric associations, of cold air mesoscyclones in the Australasian sector. *J. Geophys. Res.,* **102,** 13 873–13 887.

Carrasco, J. F., D. H. Bromwich, and Z. Liu, 1997a: Mesoscale cyclone activity over Antarctica during 1991. 1. Marie Byrd Land. *J. Geophys. Res.,* **102,** 13 923–13 937.

——, ——, and ——, 1997b: Mesoscale cyclone activity over Antarctica during 1991. 2. Near the Antarctic Peninsula. *J. Geophys. Res.,* **102,** 13 939–13 954.

Chunchuzov, I., P. W. Vachon, and B. Ramsay, 2000: Detection and characterization of polar mesoscale cyclones in RADARSAT synthetic aperture radar images of the Labrador Sea. *Can. J. Remote Sens.,* **26,** 213–230.

Douglas, M. W., M. A. Shapiro, L. S. Fedor, and L. Saukkonen, 1995: Research aircraft observations of a polar low at the east Greenland ice edge. *Mon. Wea. Rev.,* **123,** 5–15.

Grønås, S., and N. G. Kvamstø, 1995: Numerical simulations of the synoptic conditions and development of Arctic outbreak polar lows. *Tellus,* **47A,** 797–814.

Heinemann, G., and C. Claud, 1997: Meeting summary: Report of a workshop on ''theoretical and observational studies of polar lows'' of the European Geophysical Society Polar Lows Working Group. *Bull. Amer. Meteor. Soc.,* **78,** 2643–2658.

Locatelli, J. D., P. V. Hobbs, and J. A. Werth, 1982: Mesoscale structures of vortices in polar air streams. *Mon. Wea. Rev.,* **110,** 1417–1433.

Mailhot, J., D. Hanley, B. Bilodeau, and O. Hertzman, 1996: A numerical case study of a polar low in the Labrador Sea. *Tellus,* **48A,** 383–402.

Minor, T., P. J. Sousounis, J. Wallman, and G. Mann, 2000: Hurricane Huron. *Bull. Amer. Meteor. Soc.,* **81,** 223–236.

Monaldo, F., 2000: The Alaska SAR demonstration and near-real-time synthetic aperture radar winds. *John Hopkins APL Technical Digest,* Vol. 21, No. 1, 75–79.

Monteverdi, J. P., 1976: The single air mass disturbance and precipitation characteristics at San Francisco. *Mon. Wea. Rev.,* **104,** 1289–1296.

Mourad, P. D., 1996: Inferring multiscale structure in atmospheric turbulence using satellite-based SAR imagery. *J. Geophys. Res.,* **101,** 18 433–18 449.

——, 1999: Footprints of atmospheric phenomena in synthetic aperture radar images of the ocean surface—A review. *Air-Sea Exchange: Physics, Chemistry, and Dynamics,* G. L. Geernaert, Ed., Kluwer Academic, 269–290.

NRC, 1996: *The Bering Sea Ecosystem.* National Research Council, National Academy Press, 307 pp.

Orlanski, I., 1975: A rational subdivision of scales of atmospheric processes. *Bull. Amer. Meteor. Soc.,* **56,** 527–530.

Pichel, W., and P. Clemente-Colón, 2000: NOAA CoastWatch SAR applications and demonstration. *Johns Hopkins APL Technical Digest,* Vol. 21, No. 1, 49–57.

Rasmussen, E. A., 1989: A comparative study of tropical cyclones and polar lows. *Polar and Arctic Lows,* P. F. Twitchell, E. A. Rasmussen, and K. L. Davidson, Eds., A. Deepak, 47–80.

Sikora, T. D., G. S. Young, R. C. Beal, and J. B. Edson, 1995: Use of *ERS-1* synthetic aperture radar imagery of the sea surface in detecting the presence and structure of the convective marine atmospheric boundary layer. *Mon. Wea. Rev.,* **123,** 3623–3632.

——, K. S. Friedman, W. G. Pichel, and P. Clemente-Colón, 2000: Synthetic aperture radar as a tool for investigating polar mesoscale cyclones. *Wea. Forecasting,* **15,** 745–758.